NASA TECHNICAL NOTE

NASA TN D-4665

NASA TN D-4665

EXPERIMENTAL VERIFICATION OF SCALE FACTORS FOR PARAWING OPENING CHARACTERISTICS

by David L. Eichblatt, Robert H. Moore, and Richard L. Barton

Manned Spacecraft Center
Houston, Texas

NATIONAL AERONAUTICS AND SPACE ADMINISTRATION • WASHINGTON, D. C. • AUGUST 1968

EXPERIMENTAL VERIFICATION OF SCALE FACTORS FOR PARAWING OPENING CHARACTERISTICS

By David L. Eichblatt, Robert H. Moore, and Richard L. Barton

Manned Spacecraft Center
Houston, Texas

NATIONAL AERONAUTICS AND SPACE ADMINISTRATION

For sale by the Clearinghouse for Federal Scientific and Technical Information
Springfield, Virginia 22151 – CFSTI price $3.00

ABSTRACT

The verification of an analytical scaling technique by experimental drop tests under controlled conditions is presented in which the opening characteristics of a full-scale flexible parawing are predicted from the results of model testing. The scaling method is derived from a comparison of similar forces (in the equation of motion) on a scale model with a keel length of 4 feet and a full scale of 8 feet. Initial velocities of 17 to 40 feet per second were used in the test program. Test results within the scope of the program indicate that the models can be used to predict full-scale deployment characteristics.

CONTENTS

TABLES

FIGURES

EXPERIMENTAL VERIFICATION OF SCALE FACTORS FOR PARAWING OPENING CHARACTERISTICS

By David L. Eichblatt, Robert H. Moore,
and Richard L. Barton
Manned Spacecraft Center

SUMMARY

The experimental results of drop tests under controlled conditions are presented, which verify an analytical-scaling technique whereby the opening characteristics of lifting-type parachutes are predicted from the results obtained from model testing. Dynamic similarity is acquired by comparing the forces (in the equation of motion) on a scale model to similar forces on a prototype.

Two all-flexible parawings were tested; a half-scale model with a keel length of 4 feet and a payload of 4 pounds, and a full-scale model with a keel length of 8 feet and a payload of 32 pounds. These dimensions and weights were scaled to each other to obtain the corresponding dynamic similarity. The parawings were constructed from the same material, which made it necessary to correct canopy weight by the addition of ballast to the full-scale system. The parawings were deployed from an initial-packed condition and at initial velocities ranging from 17 to 40 feet per second. Although unavoidable dispersions resulted between individual drops, the averaged results of measured opening characteristics of the half-scale model were scaled according to the analytical technique to predict the full-scale results. A comparison between the prediction and the measured full-scale results confirmed the value of model scaling on the deployment characteristics of parawings.

INTRODUCTION

With the exception of their opening characteristics, the results of model testing have been most useful in the early design of full-scale parachutes. Until a recent analytical technique was developed, model opening characteristics were not applicable to full-scale opening characteristics because of the lack of an acceptable scaling method. The new technique is a method whereby dynamic similarity is obtained by comparing similar forces in the equation of motion. To confirm the scaling technique (ref. 1), experimental tests were performed using a conventional parachute dropped in an initial-reefed condition and at an initial velocity of zero. An extension to these findings is presented in this report which includes the confirmation of the scaling technique applied to a lifting-type parachute (parawing) dropped from an initial-packed condition and at various initial velocities other than zero.

Two all-flexible parawings were tested: a half-scale model with a keel length of 4 feet and a payload of 4 pounds, and a prototype with a keel length of 8 feet and a payload of 32 pounds. A significant problem was encountered in the design and construction of the parawings, a problem which greatly affected the weight and required the addition of ballast to the full-scale system. The problem was caused because canopy-cloth weights could not be scaled successfully. For example, the full-scale canopy was constructed from one of the available standard-weight parachute cloths, and the results of scaling required the model canopy to be very thin, which was both impractical and out of the range of standard-weight cloth.

For simplicity, the parawing canopies (both model and full scale) used in the test program were constructed from parachute cloth with an identical weight-per-unit area. However, the model canopy was too heavy when analytically scaled relative to the full-scale canopy. Therefore, a ballast weight was added to the full-scale parawing-payload system to compensate for the light weight of the canopy.

The model was deployed several times each at velocities of 17.9, 23.4, and 28.4 feet per second and tension-time histories were recorded. The velocities were obtained at the instant of canopy extraction. The results were scaled according to theory to predict the full-scale results. The prototype was also tested in the same manner at velocities of 25.4, 33.0, and 40.0 feet per second.

SYMBOLS

CF	correction factor
C_D	drag coefficient
C_L	lift coefficient
D	drag force, lb
d	diameter, ft
E	elongation, percent
F	force, lb
g	gravity, lb/slugs
K	spring constant, lb/in.
m	mass, slugs
$\dot{m}$	mass flow, slugs/sec
N	force scale factor

P	permeability, ft^3/ft^2-min at 0.5 in. water differential pressure
p	peak tension
q	dynamic pressure, lb/ft^2
R	ratio
S	projected area, ft^2
T	riser tension, lb
t	time, sec
V	volume, ft^3
v	velocity, ft/sec
$\dot{v}$	acceleration, ft/sec^2
W	weight, lb
x	distance, ft
ρ	atmospheric density, $slugs/ft^3$
ρ_s	structural density, $slugs/ft^3$

Subscripts:

f	full scale
m	model
PL	payload

THEORY

Reference 1 presents a derivation of the scale factors applied to a nonlifting parachute. A summary of the theory developed in reference 1 is given here for both clarity and ease of presentation. Applying Newton's second law to the vertical motion yields

$$\sum F = \frac{d}{dt}(mv) = m\dot{v} + \dot{m}v = W - D \qquad (1)$$

Applying the laws of dynamic similarity to theoretical scaling, all forces in the model equation of motion must be scaled to the same force in the full-scale equation of motion

$$\frac{(m\dot{v})_m}{(m\dot{v})_f} = \frac{(\dot{m}v)_m}{(\dot{m}v)_f} = \frac{W_m}{W_f} = \frac{D_m}{D_f} = N \tag{2}$$

or

$$R_m R_{\dot{v}} = R_{\dot{m}} R_v = R_w = R_D = N \tag{3}$$

where N represents the force scale factor equal to each of the force ratios.

To obtain the force scale factor in its most basic form, the weight scale is expanded to yield

$$R_W = R_m R_g = R_{\rho_s} R_V R_g = R_{\rho_s} R_d^3 R_g = N \tag{4}$$

Refer to reference 1 for a more extensive derivation.

The lifting force must be scaled for lifting parachutes. Aerodynamic-lift forces acting on the model and full-scale equated to equation (2) yield

$$\frac{(qSC_L)_m}{(qSC_L)_f} = N \tag{5}$$

or

$$R_q R_S R_{C_L} = R_{\rho_s} R_g R_d^3 \tag{6}$$

Solving for the ratio of the model to full-scale lift coefficient yields

$$R_{C_L} = \frac{R_{\rho_s} R_g R_d^3}{R_\rho R_v^2 R_d^2} = \frac{R_{\rho_s} R_g R_d^3}{R_\rho R_g R_d R_d^2} = 1 \tag{7}$$

where $R_{\rho_s} = R_\rho$ (ref. 1). Therefore, the model and full-scale lift coefficients must be equal, as the drag coefficients must be equal.

Table I is the result of the analytical prediction for all factors concerned. The test-condition column is tabulated because gravity and density ratios are assumed to be equal to 1.0 throughout the program. Scale factors for cloth permeability, suspension-line percent elongation, and spring constant are given. These properties are included although they were not considered as a scaling basis within the scope of the test program.

PARAWINGS AND TESTING COMPONENTS

The tests for the opening characteristics of the parawing were performed in the Vibration and Acoustics Laboratory at the Manned Spacecraft Center, Houston, Texas. The building allowed constant indoor-atmospheric conditions for the many required and repeatable deployments, and provided an unobstructed height of 85 feet for the free-fall drops. The two all-flexible parawings tested were a half-scale model with a keel length of 4 feet and a full-scale prototype with a keel length of 8 feet. For simplicity, the keel lengths were chosen as the reference base length for all linear dimensions, including the linear displacements involved in the solutions of velocities and accelerations for either parawing.

Components of the parawing-payload system (fig. 1) included the canopy, the suspension lines, a fitting for the suspension-line attach point, the load cell, and the shot bag. Test components included the ceiling-attach line, an automatic-release mechanism, a canopy-packing sleeve, a free-fall control line, and the time-load recording apparatus.

Parawing

The material used for the parawings was not scaled because the limited range of materials made it impossible to do so, and the requirement for scaling was considered negligible. Each parawing canopy was constructed of 2 oz/yd^2 of low porosity (3.5 ft^3/ft^2-min at 0.5 in. of water differential pressure) rip-stop nylon cloth cut identically in shape, but scaled differently in overall dimension by definite ratios.

TABLE I. - SCALE FACTORS

Quantity	Ratio	Result	Test condition
Diameter	R_d	R_d	R_d
Area	R_S	R_d^2	R_d^2
Volume	R_V	R_d^3	R_d^3
Gravity	R_g	R_g	1.0
Density	R_ρ	R_ρ	1.0
Distance	R_x	R_d	R_d
Velocity	R_v	$R_g^{1/2}R_d^{1/2}$	$R_d^{1/2}$
Acceleration	$R_{\dot{v}}$	R_g	1.0
Time	R_t	$R_g^{-1/2}R_d^{1/2}$	$R_d^{1/2}$
Mass	R_m	$R_\rho R_d^3$	R_d^3
Mass flow	$R_{\dot{m}}$	$R_\rho R_g^{1/2}R_d^{5/2}$	$R_d^{5/2}$
Weight	R_W	$R_\rho R_g R_d^3$	R_d^3
Drag coefficient	R_{C_D}	1.0	1.0
Lift coefficient	R_{C_L}	1.0	1.0
Permeability	R_P	$R_g^{1/2}R_d^{-1/2}$	$R_d^{-1/2}$
Elongation	R_E	1.0	1.0
Spring constant	R_K	$R_\rho R_g R_d^2$	R_d^2

Parawing dimensions and suspension-line lengths are given in figure 2. Suspension lines of the model were of 250-pound test, nylon cord; those of the full-scale prototype were 750-pound test.

Load-Measuring System

The load cell was a simple 3-inch diameter torus-shaped steel ring encapsulated with a strain gage. A data hardline was connected to the load cell at one end, with a multichannel strip chart connected at the other end. With this arrangement, an accurate tension-time history was recorded for each of the parawing drops.

Payload

The payloads shown in figure 1 include the total weights beginning at the center of the load cell and progressing through all components down to and including the shot bag. A breakdown of component weights for the total system of either parawing is given in table II. The full-scale system required an additional ballast to make up for the weight lost using the same weight-per-unit area canopy cloth as was used for the model. The shot bags were of nylon cloth sewn in a cylindrical shape and filled with lead shot to a weight of 3.8 pounds for the scale model, and 31.8 pounds for the full-scale parawing. The lengths and diameters of the payloads were scaled to each other in accordance with the scaling technique to obtain a corresponding aerodynamic drag, even though the drag was considered negligible in calculations.

TABLE II. - SYSTEM WEIGHTS

Component	4-foot parawing, lb	8-foot parawing, lb
Shot bag	3.80	31.80
Load cell	.30	.30
Fittings	.05	.05
Parawing weight	.30	1.70
Ballast	.00	1.64
Total weight	4.45	35.49
Scaled weight	35.60	4.44

Canopy-Packing Sleeve

Canopy-packing sleeves (deployment sleeves) were made of rubber-impregnated cotton cloth cut in a rectangular pattern. With the sleeves lying flat and with the use of pile fasteners, the parawings were enveloped and rolled into a cylindrical shape ready for deployment.

Automatic-Release Mechanism

The parawing automatic-release mechanism (fig. 3) is a hand-cocked spring-loaded cutting blade, which is released by a solenoid switch. Upon command, the cutting blade severed a light cord which tightly lashed the packed canopy to the release mechanism, thereby dropping the parawing-payload system.

DEPLOYMENT TESTS

The sequence of events involved in the preparation of a drop includes: (1) folding the canopy onto the sleeve, (2) enveloping the sleeve loosely about the canopy at such a position that the skirt of the canopy is approximately even with the bottom of the sleeve, (3) tightly lashing both the canopy and sleeve to the release mechanism at a point midway of the sleeve, and (4) lifting the entire system to predeployment elevation. Figure 4 shows the sleeve and parawing before packing. Figures 5 and 6 show the model and full-scale parawing systems positioned for deployment.

The packed parawing and its payload, when released, are allowed to free fall a specific distance to obtain a particular velocity. This velocity is termed the initial-deployment velocity throughout the tests. The free-fall distance is controlled by a draped line attached between the release mechanism and the top of the sleeve. Upon release, the system falls to the end of the line causing extraction of the canopy and, thus, commencement of opening. The sequence of events in deployment is release, free fall, extraction, commencement of opening, full opening, and transition to glide. A pictorial history of the deployment sequence for both the model and full-scale parawings is shown in figures 7 and 8.

Three series of drops were made with the scale model using free-fall control lines of 5, 8.5, and 12.5 feet. The free-fall distances caused the model canopy to initiate deployment at velocities of 17.9, 23.4, and 28.4 feet per second. Tension-time histories were recorded during all drops. The model free-fall control lines were scaled according to theory which required the full scale to have drop lengths of 10, 17, and 25 feet. These lengths yielded initial velocities of 25.4, 33.0, and 40.0 feet per second. Tension-time histories were also recorded during this series of drops.

DATA REDUCTION

Direct measurements were made of the tension-time histories. Acceleration, velocity, and distance-time histories were computed by considering the payload equation of motion in vertical descent

$$m_{PL}\dot{v} = T + D - W_{PL} \tag{8}$$

The payload drag is assumed to be negligible and the riser-line tension is assumed to act along the vertical. The riser line will remain parallel to the gravity vector until sufficient lift in the parachute has caused a measurable pitch angle. Analysis of motion-picture data indicates this occurs immediately after peak tension, after which the data-reduction equations no longer hold. Solving equation (8) for the acceleration yields

$$\dot{v} = \frac{T}{m} - g \tag{9}$$

Integration yields the velocity

$$v = \int \frac{T}{m}\, dt - gt \tag{10}$$

Integrating again yields distance

$$x = \int v\, dt = \iint \frac{T}{m}\, dt\, dt - \frac{1}{2} gt^2 \tag{11}$$

To compensate for the light weight of the full-scale canopy (caused by using the same cloth for both canopies), a ballast weight was added to the system. In most cases, the weight was attached above the load cell to simulate canopy weight. In large systems, however, adding a heavy ballast above the load cell would not be practical. Therefore, a series of drops was made to verify scaling with the ballast attached below the load cell; thus, the ballast became a part of the payload system. In this configuration, the individual payload and parawing weights do not scale correctly although their total weights do. Further, the tension measurements will not scale correctly. An approximation to rectify this condition is derived as follows. For the ideal case of no ballast, the weight ratio in the test condition is

$$R_W = R_d^{\,3} = \frac{1}{8} \tag{12}$$

With the ballast added below the load cell, the weight ratio of the payload becomes

$$\frac{1}{R_W} = \frac{0.5\left[W_{(\text{load cell})}\right] + W_{(\text{fittings})} + W_{(\text{ballast})} + W_{(\text{bag})}}{W_m} \tag{13}$$

or

$$\frac{1}{R_W} = \frac{0.15 + 0.05 + 1.64 + 31.80}{4} = 8.41 \tag{14}$$

Therefore, the correction factor is simply a ratio of this value as compared to the theoretical value; thus

$$CF = \frac{8.41}{8.0} = 1.051 \tag{15}$$

The full-scale force measurements will be 5.1 percent too high, and the model predicted forces must be increased by 5.1 percent.

RESULTS

Repeatability

Although an effort was made to minimize the scatter of data by the described methods of deployment, the spread is spontaneous and appears to be characteristic of flexible-parachute deployment. Repeatability spread is unavoidably present in each of the series of deployment tests, and is verified by the tension-time plots. The differences may be considered to be the results of a large number of very small elementary differences caused by any one or all of the following variables (ref. 2):

1. Variable friction of the sleeve to the canopy due to packing

2. The twisting and entanglement of suspension lines

3. Aerodynamic turbulence in the wake of both the free-falling payload and the suspension lines

Predicting results on the full-scale parawing from observations on the model parawing required an adequate number of drops to establish the most probable representative value. The desired degree of accuracy relative to this representative value is a function of the number of drops made. Obtaining a complete statistical description (requiring many drops) was prohibitive and was considered secondary to scaling. Based upon the degree of scatter, only four or five drops were necessary to establish the representative behavior for all cases, except the low initial-opening velocities of both parawings. More drops were made at low initial velocities to gain knowledge of the individual behavior of the parawings required for the success of the series of tests.

Scale-Model Deployment Characteristics

Figure 9 shows the scale-model deployment characteristics at low, medium, and high initial-opening velocities with measured tension plotted against time. Figure 9(a) is a diagram of 12 deployments performed at the low initial velocity of 17.9 feet per second. Before release, the tension is equal to the static-payload weight. Upon release, the tension quickly goes to zero and remains there until the opening velocity is reached (at approximately 0.8 second) when drag forces on the canopy begin to increase, thereby increasing the tension measurements. Peak tension is reached in approximately 1 second. The parawing passes through peak tension and begins transition to glide where the tension again approaches the payload weight. Figure 9(b) is similar to figure 9(a) except four drops were made, and the initial-opening velocity for each was 23.4 feet per second. Opening began at 0.9 second and peak tension occurred at approximately 1.15 seconds and then decreased. Figure 9(c) also represents four drops, but deployment was at a velocity of 28.4 feet per second. The curves have the same general shape, but they peak out at a slightly higher load. Initial opening for the high velocity of 28.4 feet per second occurs at approximately 1 second. Peak tension occurs at about 1.25 seconds.

Full-Scale Characteristics

Figure 10 represents the full-scale parawing characteristics. Figure 10(a) diagrams 14 deployments performed at an initial velocity of 25.4 feet per second. Commencement of opening for the group is approximately 1.2 to 1.4 seconds. Peak tension occurs at about 1.6 seconds. In figure 10(b), the medium velocity results (33.0 feet per second) show four drops and indicate commencement of opening at approximately 1.5 seconds with peaks at approximately 1.7 seconds. The high velocity results (40.0 feet per second) in figure 10(c) depict five drops. The opening is approximately 1.5 to 1.7 seconds with peaks at 1.7 to 2 seconds.

Averaging Technique

Since the time of occurrence of an event is of equal importance in scaling the event (in this case, peak tension), averaging was done to reflect both. By taking n number of tension-time traces, as shown in the following curves, the peak tension p is averaged as

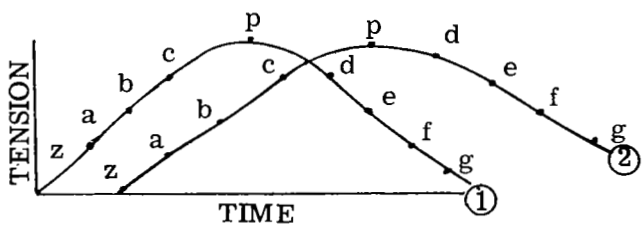

$$T_{peak,\,avg} = \frac{T_{1,p} + T_{2,p} + \ldots + T_{n,p}}{n} \qquad (16)$$

Being equally interested in when this average peak tension occurs, the time to peak is averaged by

$$t_{peak,\,avg} = \frac{t_{1,\,P} + t_{2,\,P} + \cdots + t_{n,\,P}}{n} \tag{17}$$

More than just the peak tension point is needed to evolve a representative curve. For each curve, the last point of zero tension (z) was selected, and points of similarity (a to c) between this point and the peak-tension points were selected for averaging. The tension at these points and the times of their occurrence were averaged in the same way. The negative slope of each trace was averaged (points d to g), which led to the representative curve. Also, the averaging for the acceleration, velocity, and distance-time histories was done. But with these, the time of occurrence was fixed by the times used with the tension-time histories.

Scaling Results

To predict the measured full-scale tension-time histories from the measured model results, the model data were averaged to yield one representative curve as previously described. This average curve was then used to predict the average full-scale data by multiplying the tension by the inverse of the force ratio of 8 and multiplying the time by the inverse of the time ratio of $\sqrt{2}$. Figure 11 shows the results of this comparison. The solid line is the averaged full-scale results, while the dotted line is the prediction from the average of the model data. Note that for all three velocities, the predictions from the model data match the measured results well within the repeatability of the data. The medium velocity-tension data are overpredicted, while the high and low velocity data are underpredicted. Model predictions for all vehicles indicate that the model parachutes opened slightly earlier than the full-scale parachutes. The acceleration-time histories were computed and averaged as before. The model data were used to predict the full-scale data as per the scaling ratios.

$$\left.\begin{aligned} R_V &= 1 \\ R_t &= \sqrt{\frac{1}{2}} \end{aligned}\right\} \tag{18}$$

Figure 12 compares the predicted and averaged acceleration-time histories. The results indicate that the model acceleration data can be used to predict the full-scale data. After peak negative acceleration, the data reduction equations do not account for the observed lift. In the same manner, figures 13 and 14 were constructed to compare the velocity-time and distance-time histories. All differences become less and less pronounced as the integration averages out the differences. The model results accurately predict the full-scale data. Again, the observed lift after the time of peak tension caused some error in the results.

Full-Scale Characteristics with Repositioned Ballast Weight

Because it was necessary to use a ballast weight in the full-scale parawing system, an investigation was made to determine the effects of positioning the ballast above the load cell (simulating canopy weight) or below the load cell (adding to the tension measurements). A series of drops was made for both cases. Figure 10 shows the results when the ballast was above the load cell. Figure 15 shows the results when the ballast was below the load cell. The model results, averaged and scaled up for comparison in figure 11(a), were corrected for the additional weight of ballast by the derived correction factor. The prediction was then plotted with the average of the full-scale series of figure 15 with the comparison shown in figure 16. Note that the model results satisfactorily predict full-scale tensions with the ballast below the load cell. Thus, the conclusion is that the inability to scale the canopy weight can be compensated for by altering the payload weight (below the load cell) a corresponding amount, and then correcting the measured results.

CONCLUDING REMARKS

The limp characteristics of these parawing systems make it virtually impossible to duplicate precisely a given deployment test. Throughout the program, the results were invariably random. However, in most cases the results assumed the same general shape. Despite poor repeatability, the described technique of model scaling can predict the opening characteristics with sufficient accuracy to be useful in parawing design.

The conclusions are summarized as follows:

1. Model-parawing-deployment characteristics can predict full-scale deployment characteristics.

2. The inability to scale the model canopy weights can be compensated for by adjusting the weight distribution of the parawing system.

Manned Spacecraft Center
National Aeronautics and Space Administration
Houston, Texas, May 7, 1968
961-21-30-09-72

REFERENCES

1. Barton, Richard L.: Scale Factors For Parachute Opening. NASA TN D-4123, 1967.

2. Gray, J. Harvey: Attenuation of Deployment and Opening Forces of Certain Aerodynamic Decelerators. Paper presented at Symposium on Parachute Technology and Evaluation (Edwards Air Force Base, Calif.), Technical Documentary Report No. 64-12, FTC-TDR-64-12, Sept. 1964.

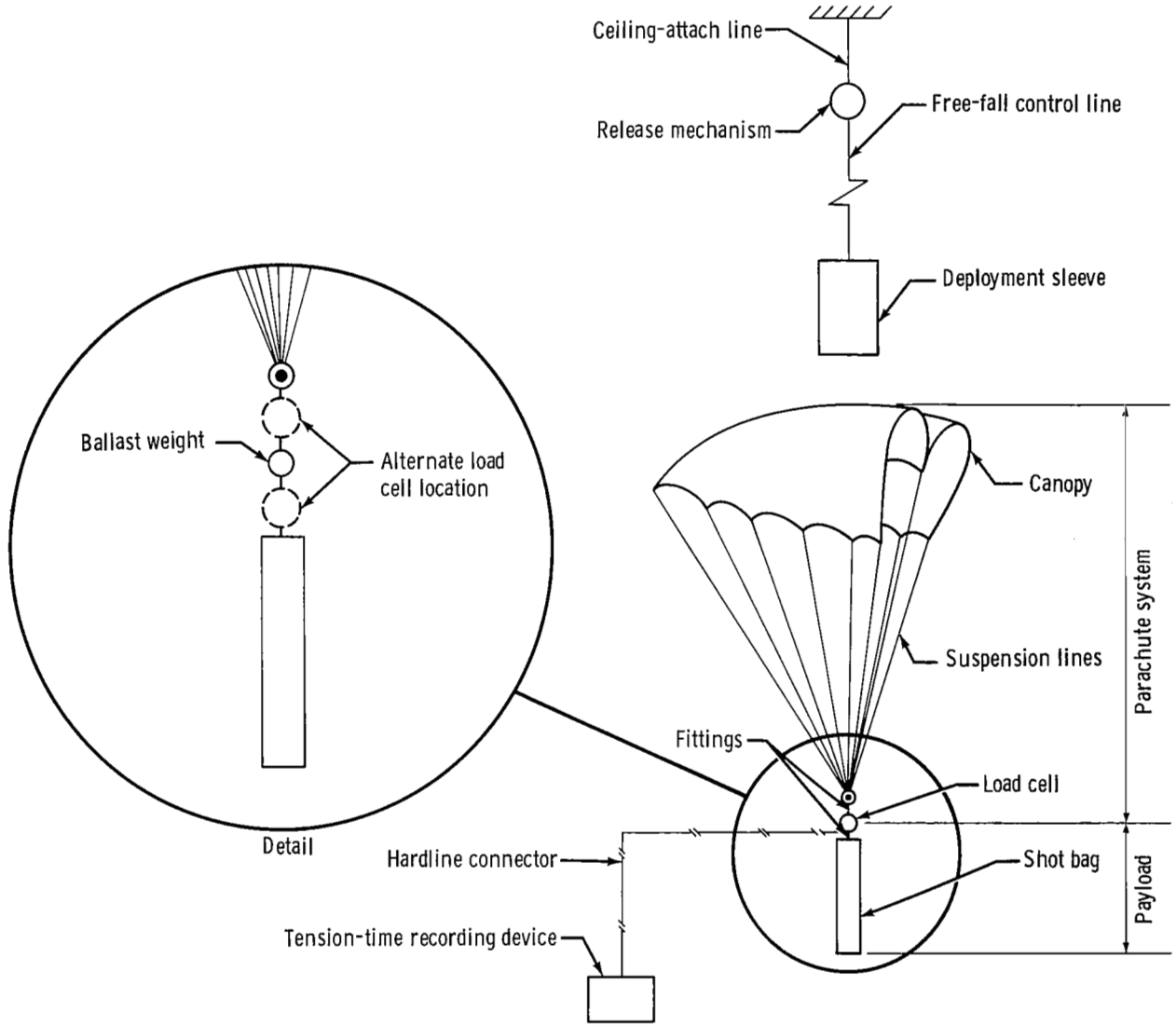

Figure 1. - General parawing payload with testing components.

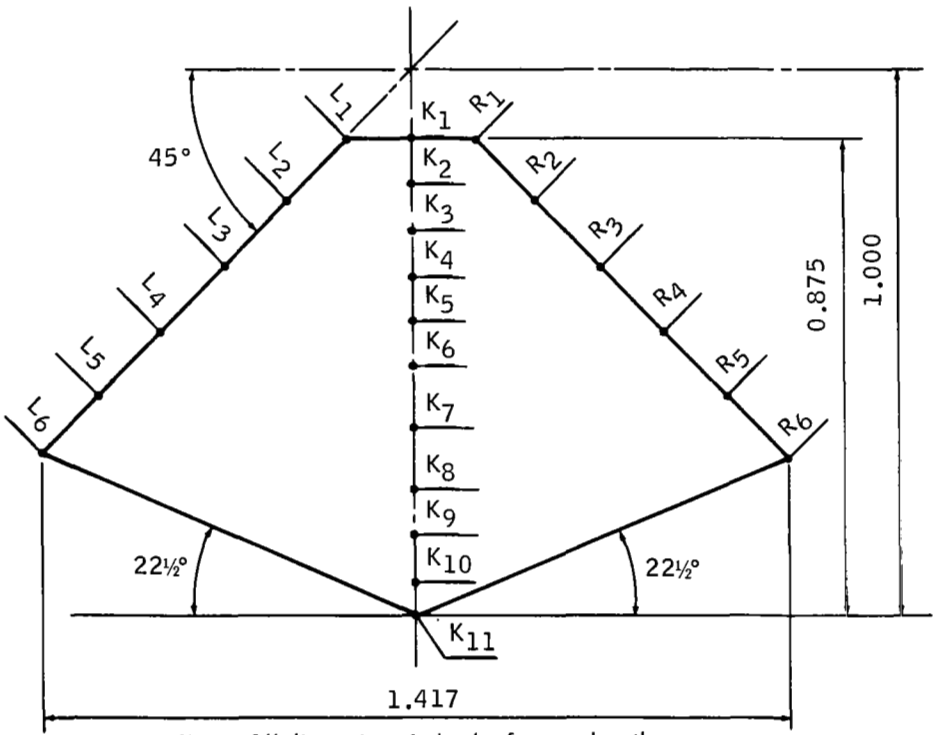

Note: All dimensions in keel reference length

Line	Line length	Distance from leading edge
R_1 & L_1	1.333	0.177
R_2 & L_2	1.281	0.333
R_3 & L_3	1.237	0.500
R_4 & L_4	1.167	0.667
R_5 & L_5	1.119	0.833
R_6 & L_6	1.001	1.000
K1	1.292	0.125
K_2	1.315	0.208
K_3	1.325	0.292
K_4	1.304	0.375
K_5	1.279	0.458
K_6	1.271	0.542
K_7	1.271	0.646
K_8	1.271	0.750
K_9	1.256	0.833
K_{10}	1.180	0.917
K_{11}	1.094	1.000

Figure 2. - Parawing canopy planform.

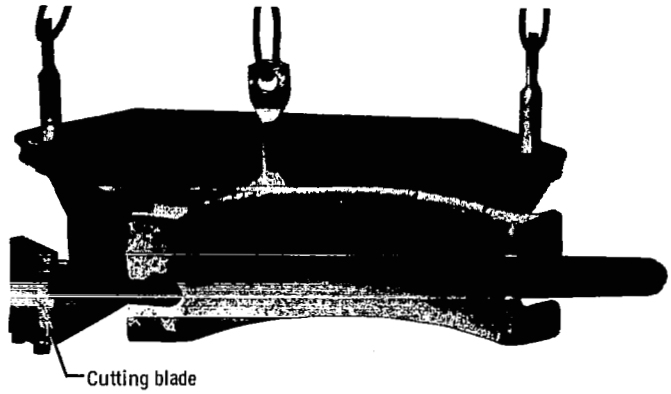

(a) Side view showing cutting blade cocked.

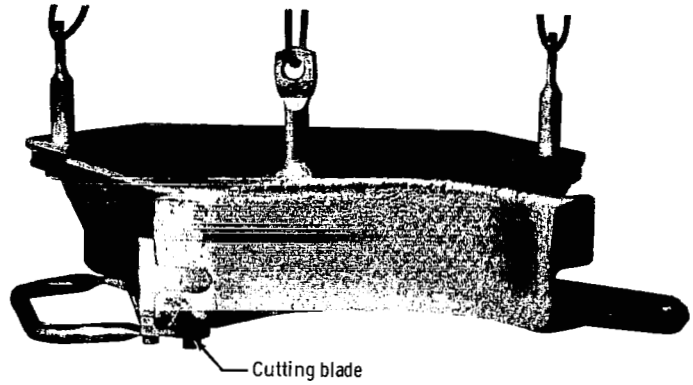

(b) Side view showing cutting blade in closed position.

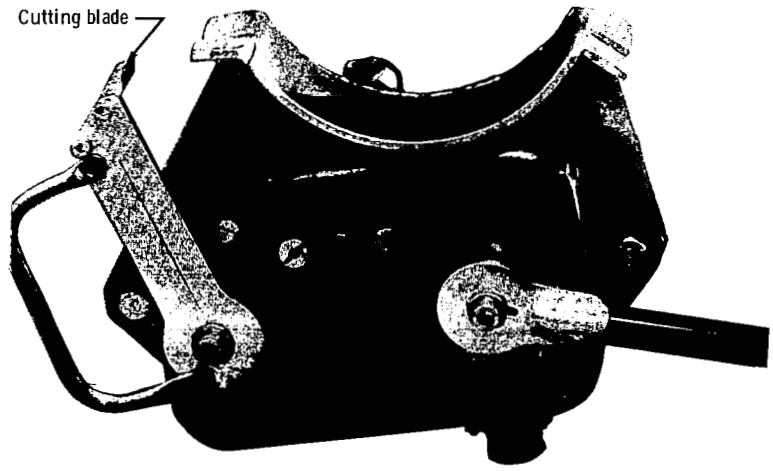

(c) Bottom view showing cutting blade cocked.

Figure 3. - Automatic release mechanism.

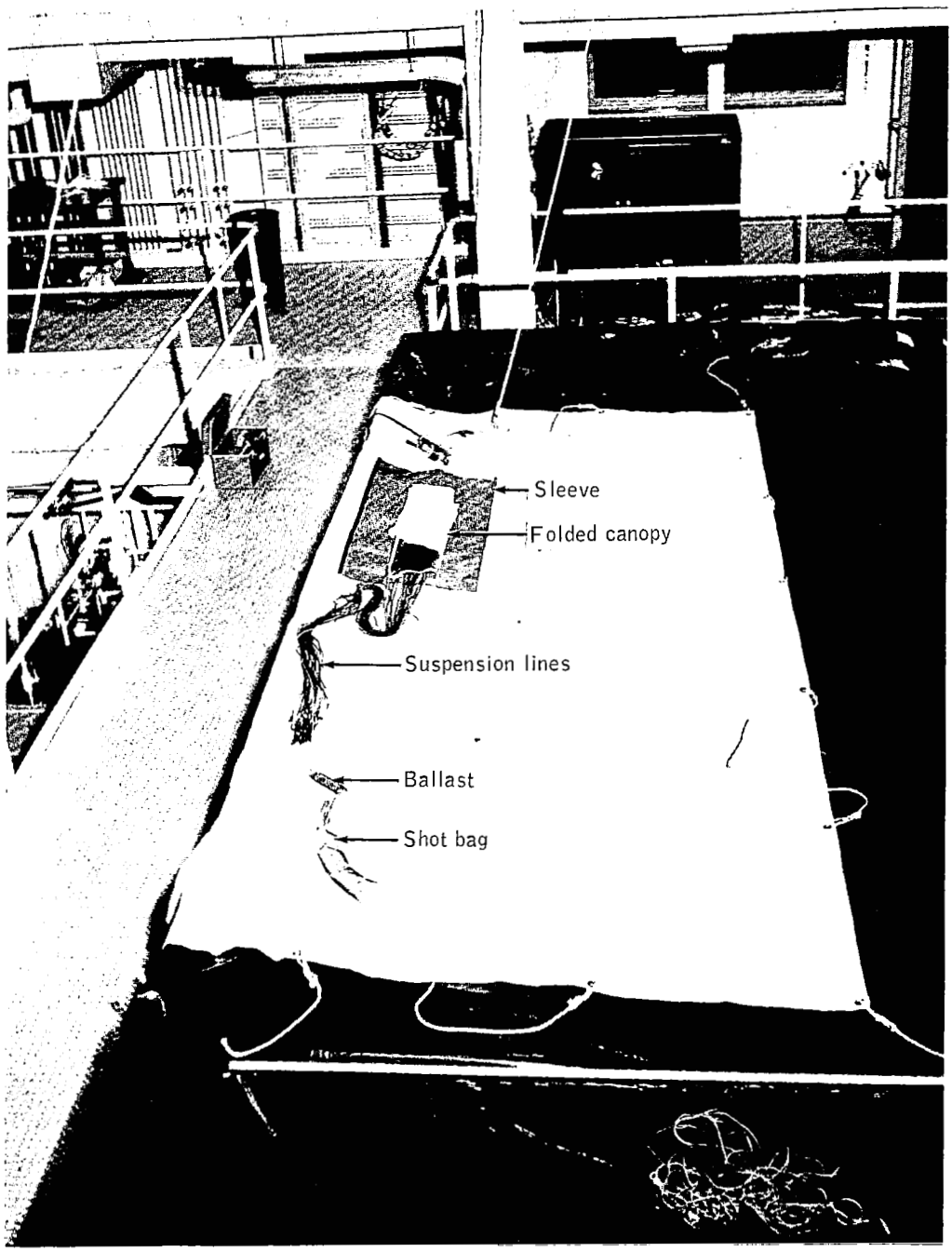

Figure 4. - Parawing folding and packing layout (full scale).

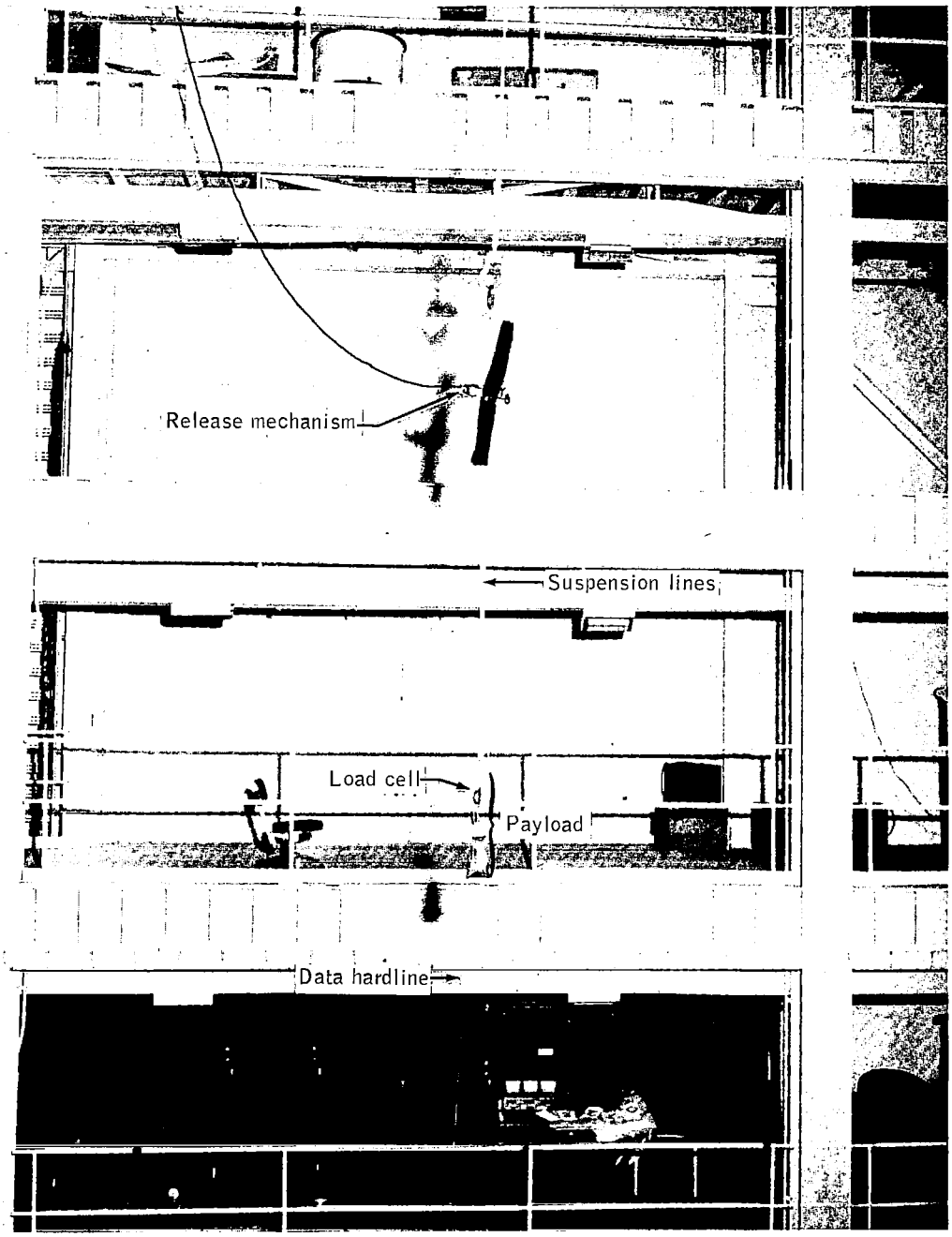

Figure 5. - Model parawing positioned for deployment.

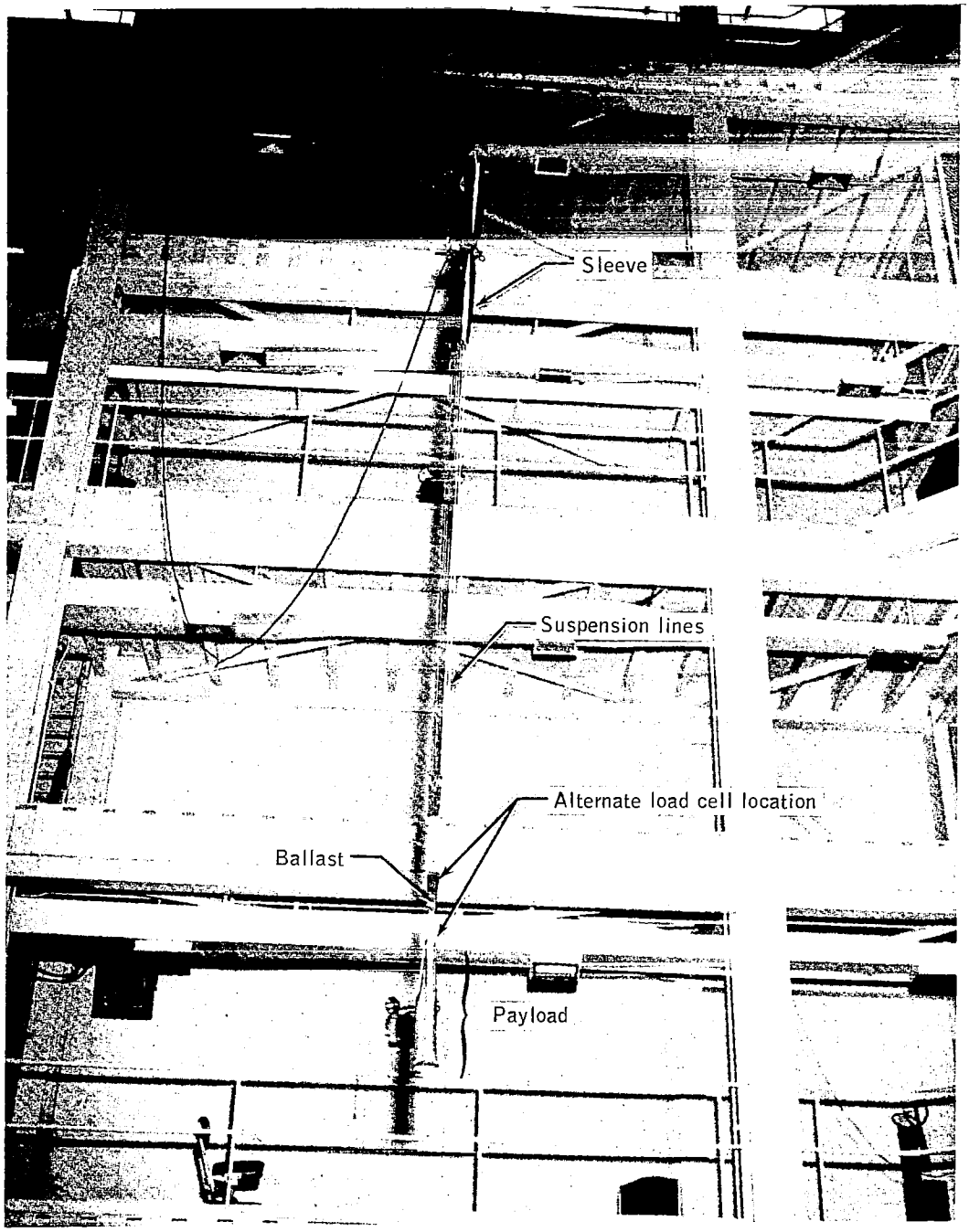

Figure 6. - Full-scale parawing positioned for deployment.

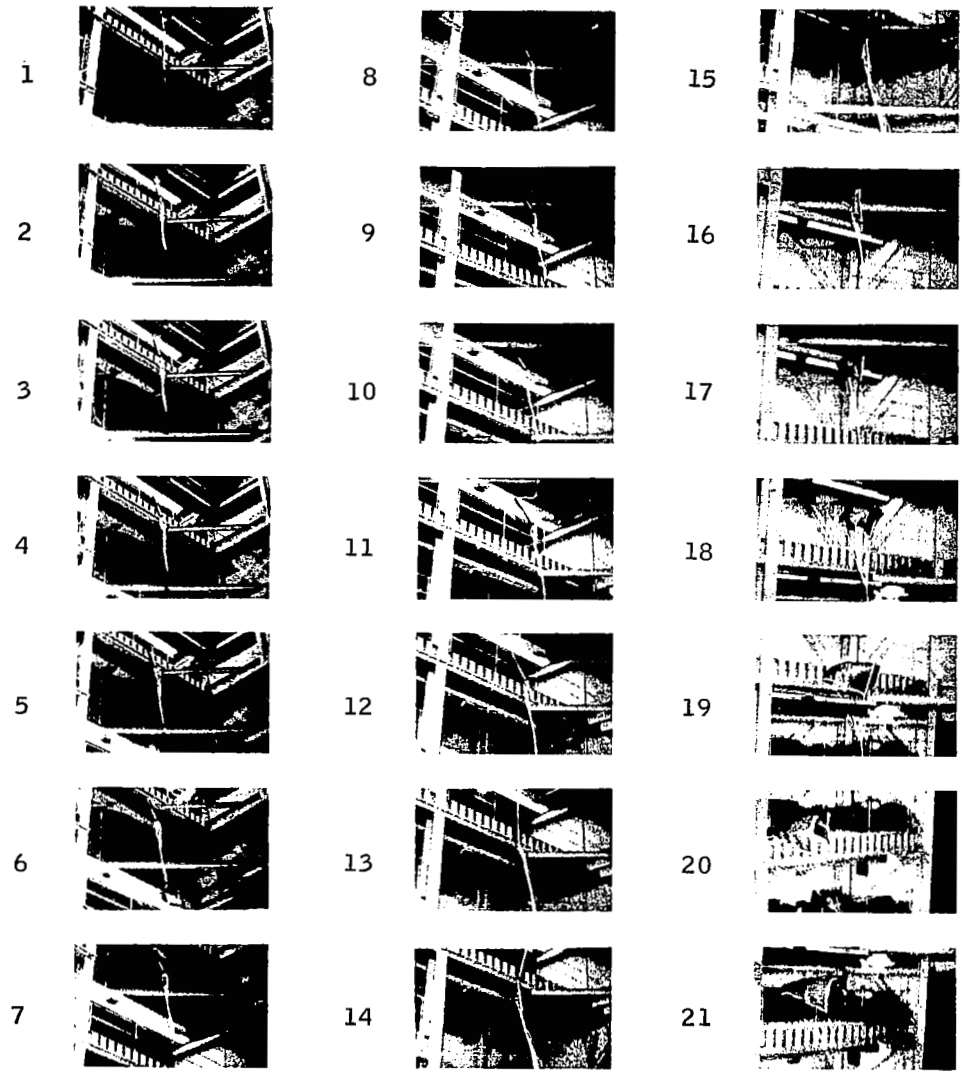

Figure 7. - Deployment sequence of model parawing.

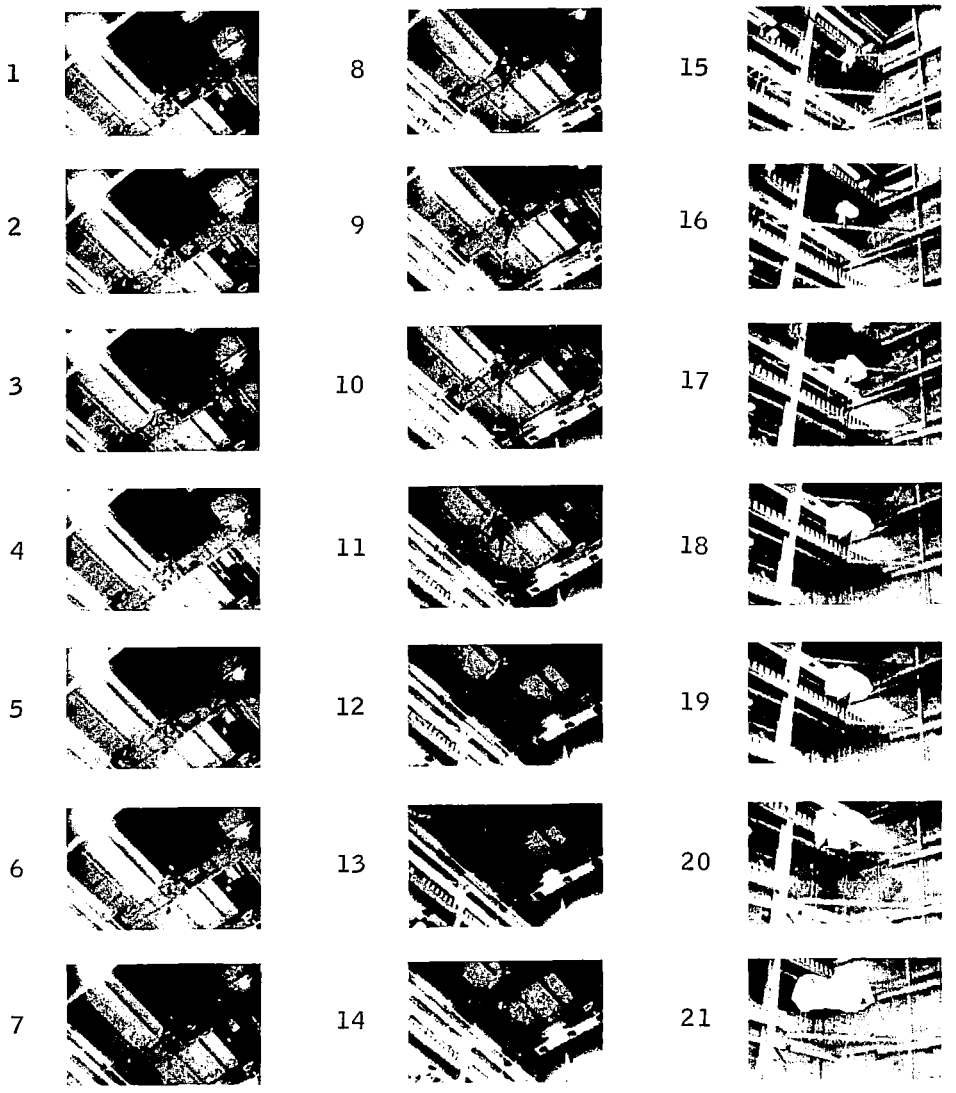

Figure 8. - Deployment sequence of full-scale parawing.

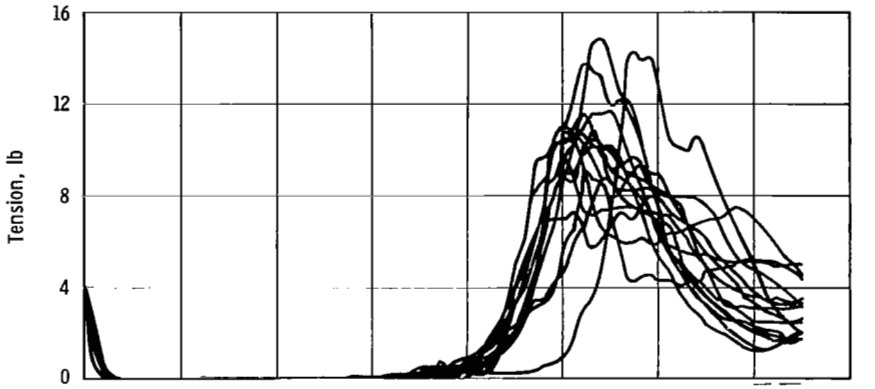

(a) Low velocity (17.9 ft/sec).

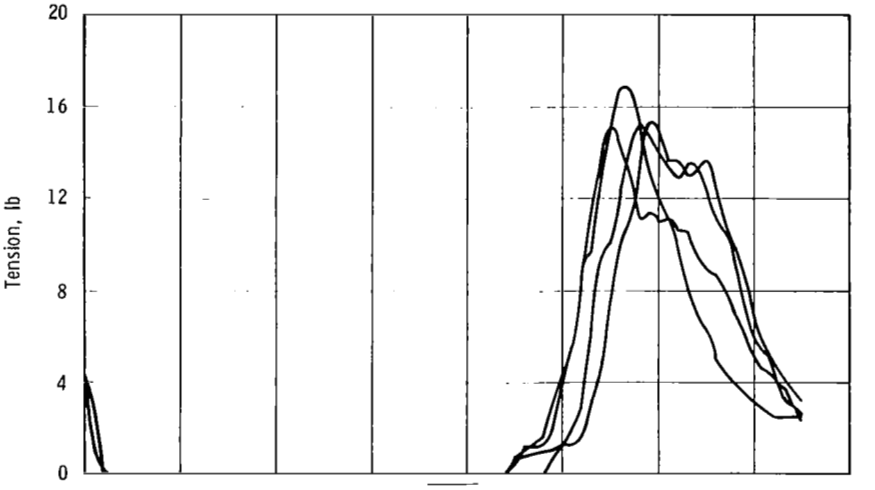

(b) Medium velocity (23.4 ft/sec).

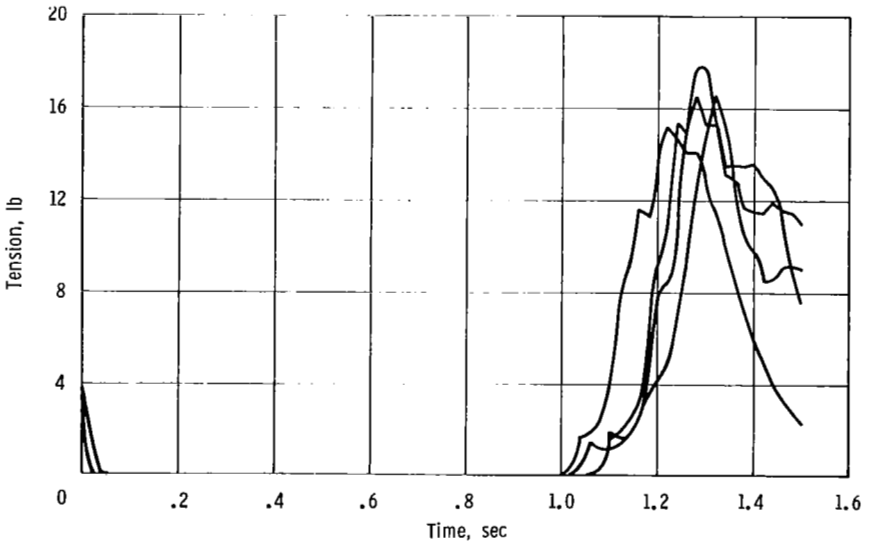

(c) High velocity (28.4 ft/sec).

Figure 9. - Scale-model deployment characteristics.

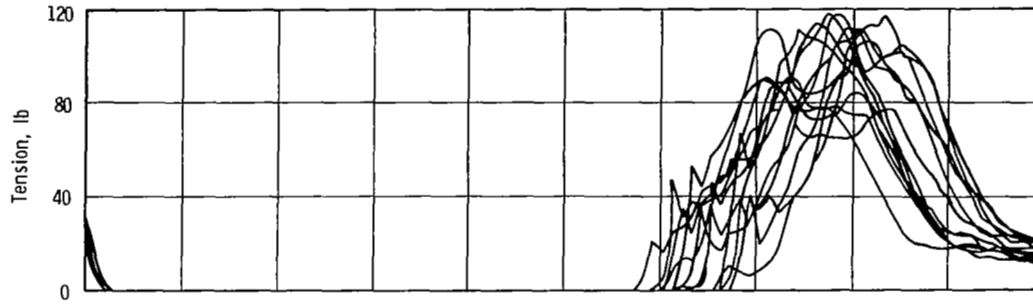

(a) Low velocity (25.4 ft/sec).

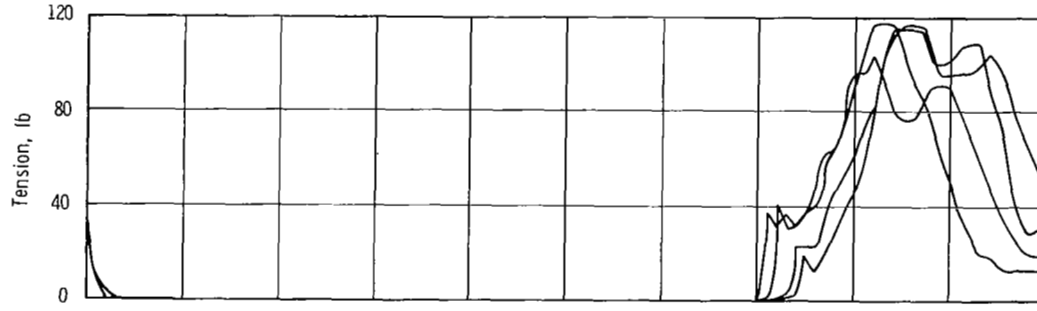

(b) Medium velocity (33.0 ft/sec).

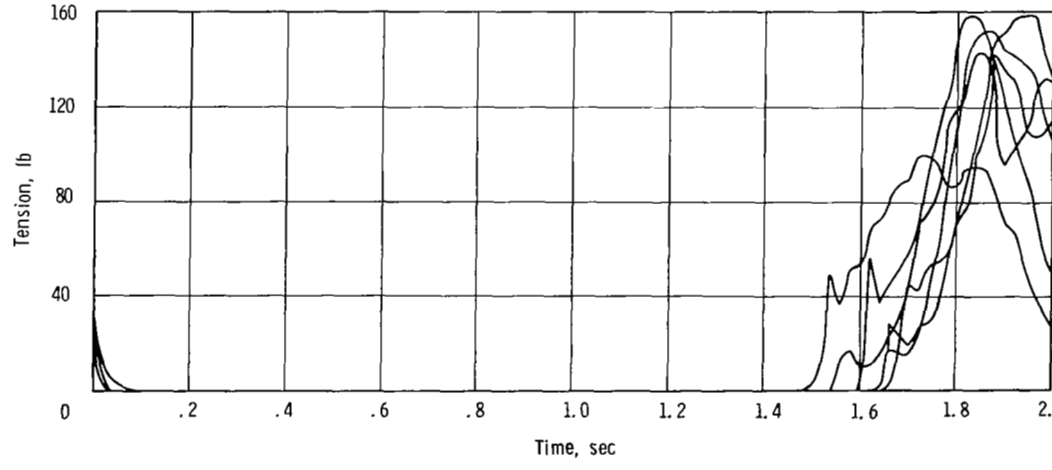

(c) High velocity (40.0 ft/sec).

Figure 10. - Full-scale deployment characteristics.

(a) Low velocity (25.4 ft/sec).

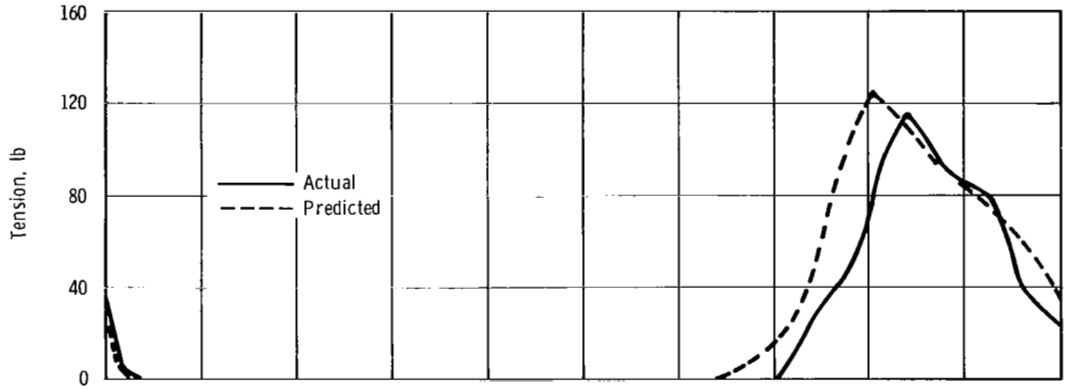

(b) Medium velocity (33.0 ft/sec).

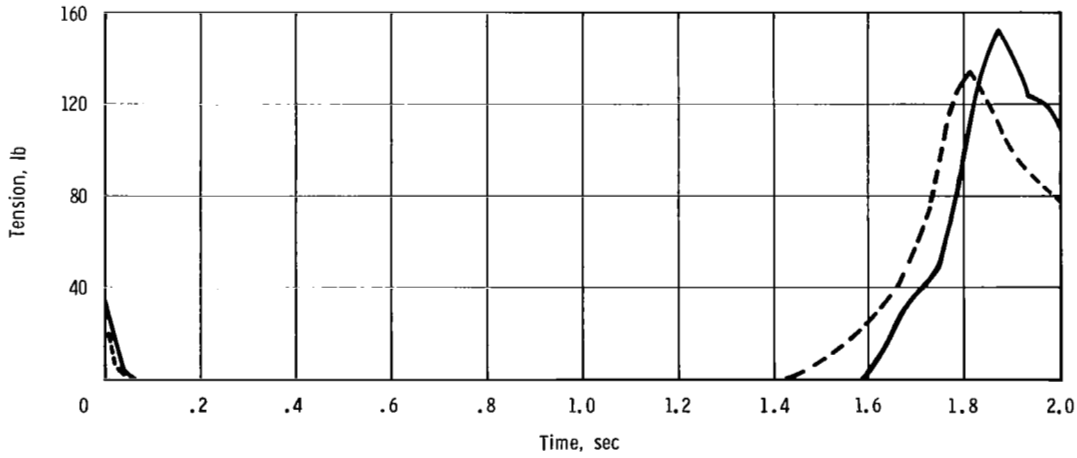

(c) High velocity (40.0 ft/sec).

Figure 11. - Comparison of predicted and actual average tension-time histories.

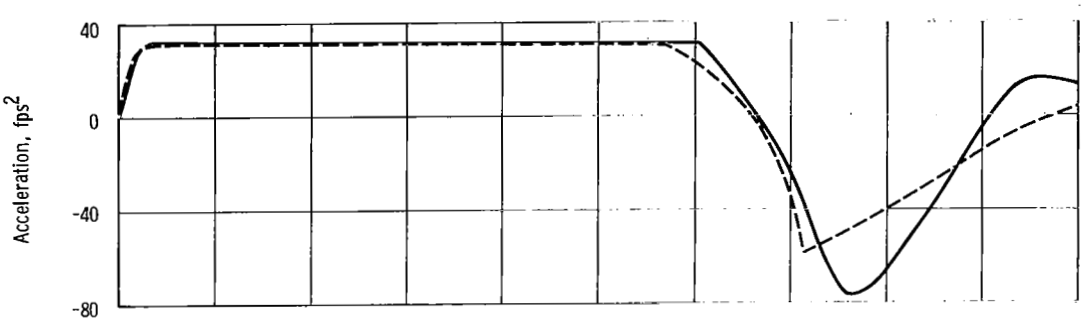

(a) Low velocity (25.4 ft/sec).

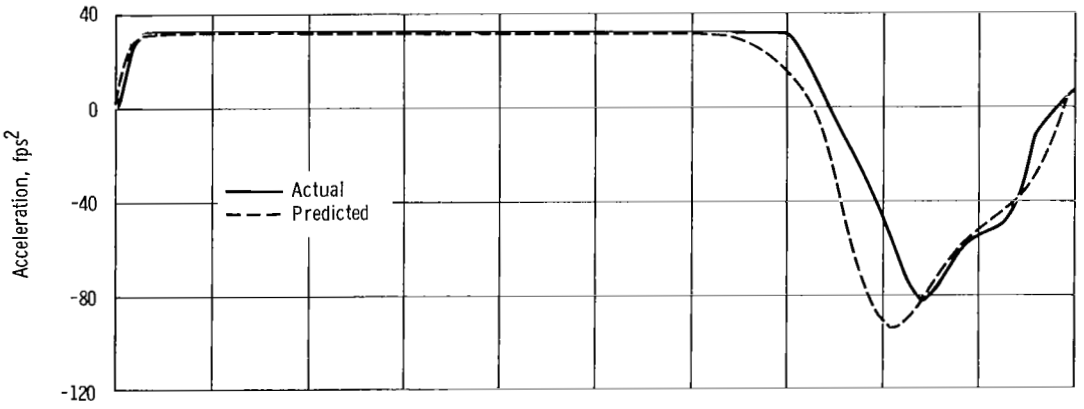

(b) Medium velocity (33.0 ft/sec).

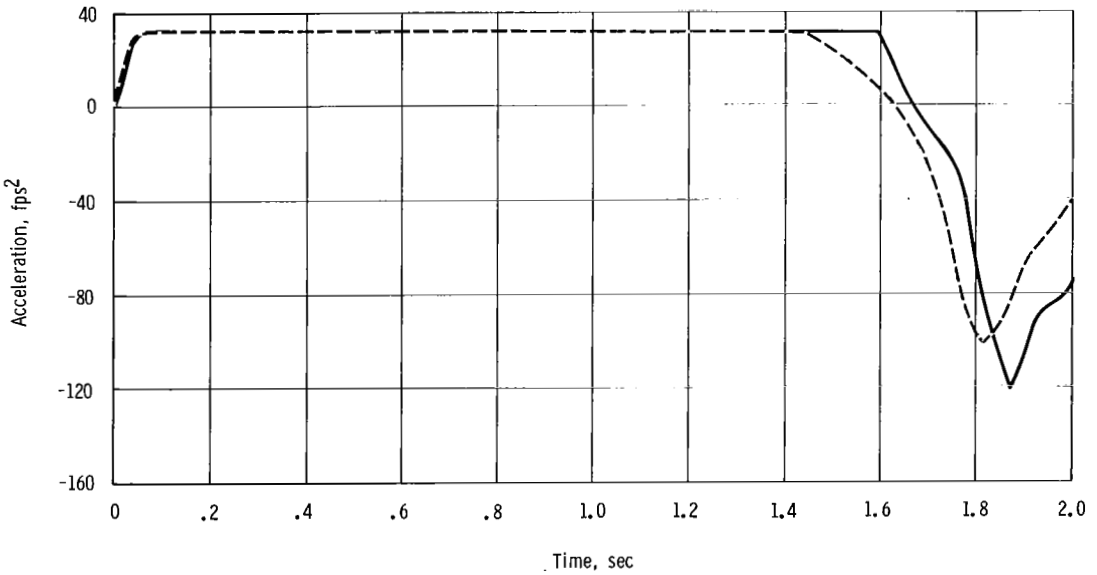

(c) High velocity (40.0 ft/sec).

Figure 12. - Comparison of predicted and actual average acceleration-time histories.

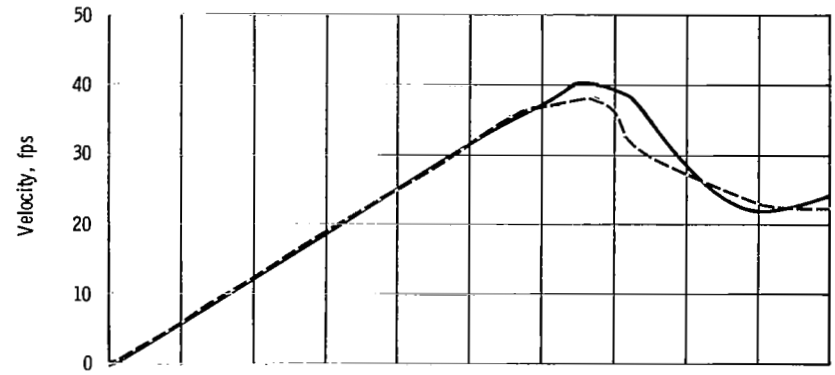

(a) Low velocity (25.4 ft/sec).

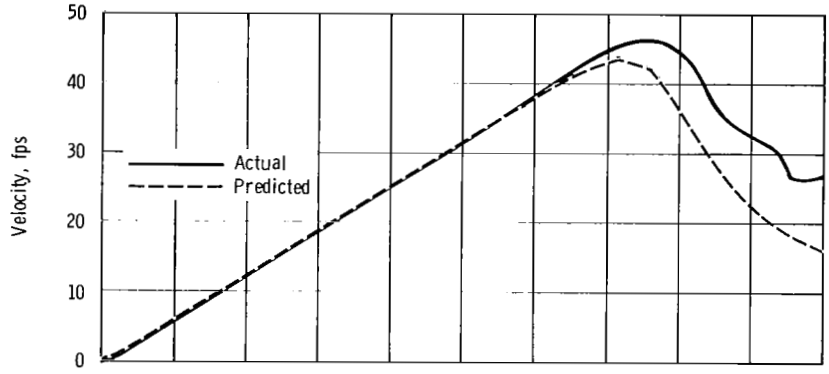

(b) Medium velocity (33.0 ft/sec).

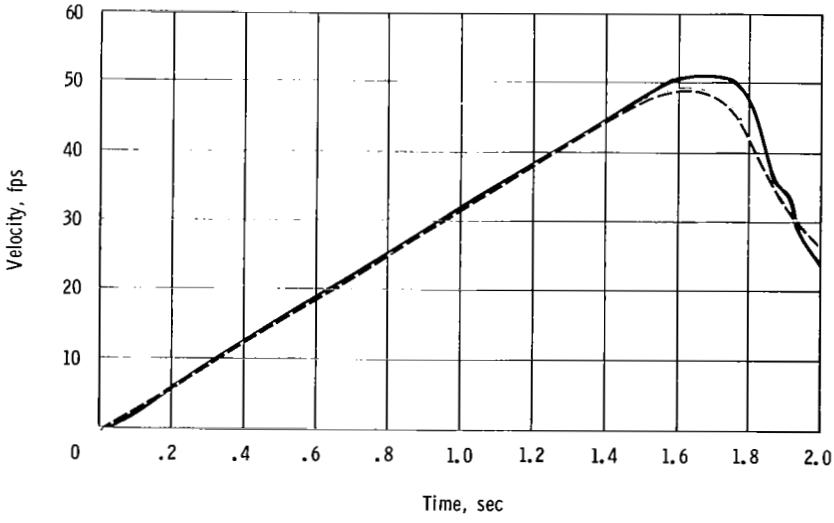

(c) High velocity (40.0 ft/sec).

Figure 13. - Comparison of predicted and actual average velocity-time histories.

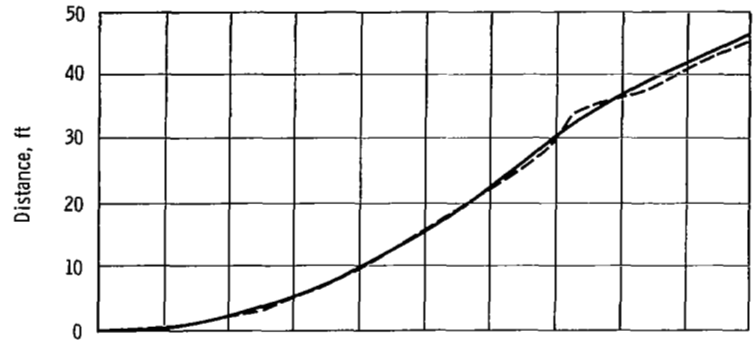

(a) Low velocity (25. 4 ft/sec).

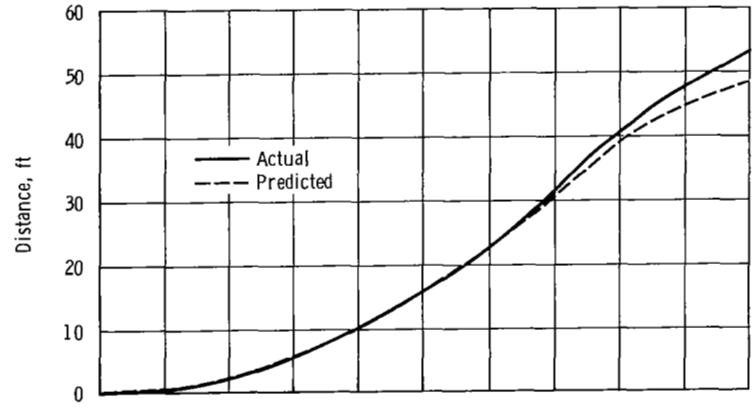

(b) Medium velocity (33. 0 ft/sec).

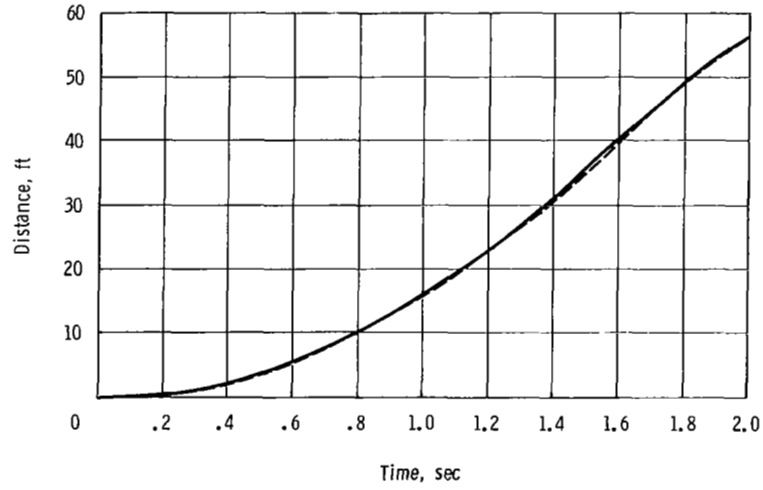

(c) High velocity (40. 0 ft/sec).

Figure 14. - Comparison of predicted and actual average distance-time histories.

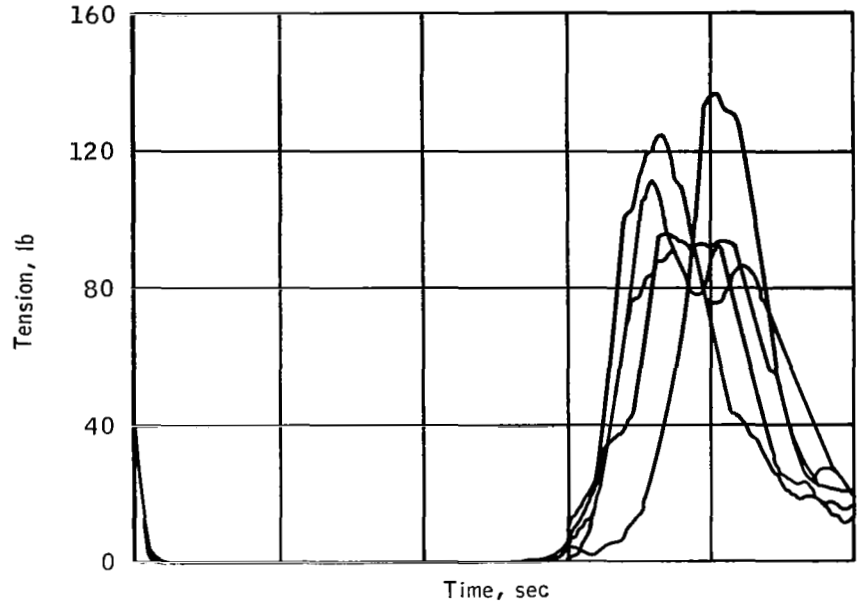

Figure 15. - Full-scale deployment characteristics (compensated canopy weight below load cell) (25.4 ft/sec).

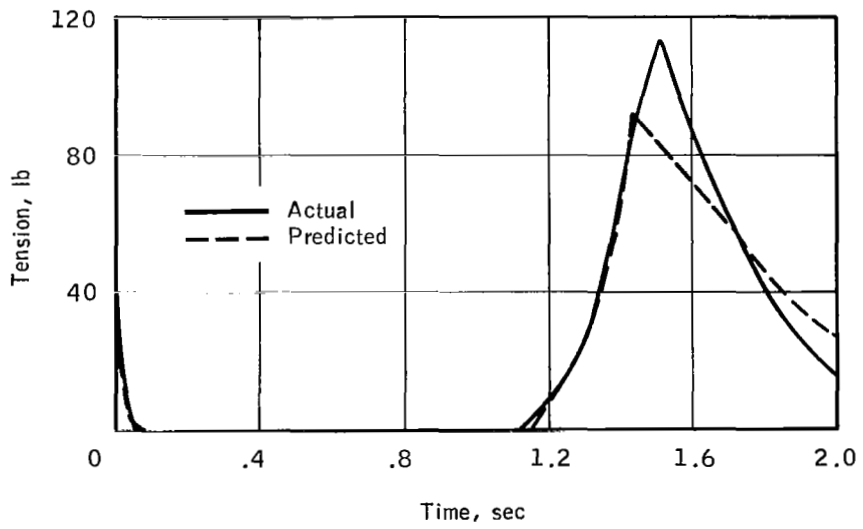

Figure 16. - Comparison of predicted and actual average tension-time histories (compensated canopy weight below load cell) (25.4 ft/sec).